USEFUL SLOT-UNIPOLE ANTENNA SYSTEMS

Kiyohiko Itoh
Faculty of Engineering, Hokkaido University, Sapporo, Japan

and

David K. Cheng
Electrical Engineering Dept., Syracuse University, Syracuse, N. Y., U.S.A.

ABSTRACT

It is well known that unipole (or monopole) and slot antennas can be used to detect electric and magnetic fields respectively. An antenna system comprising a suitable arrangement of these two types of antennas can therefore be expected to yield characteristics which would not be attainable if either type is used alone. This paper discusses the principles of operation and applications of two slot-unipole (or monopole) antenna systems. The antenna itself consists of a unipole (or monopole) and two slots mutually perpendicular to one another. It will be shown that, together a suitable processing circuitry, the antenna can be made (A) to serve as a receptor of electromagnetic energy density, or (B) to yield a cardioid pattern with an adjustable null location. Both of these two features have important practical applications.

PART A* ENERGY DENSITY ANTENNA

I. INTRODUCTION

First of all, we would like to explain about the combination of slot-unipole antenna system and its processing circuit, as shown in Fig. 1 and 2. In Fig. 2, the output of the summing amplifier is proportioned to the energy density of the wave intercepted by the slot-unipole antenna system. Therefore, this combination forms an energy density antenna system that samples the electromagnetic energy density in space.

Interference between incident and reflected signals in mountainous regions or cities with high buildings creates spatial standing-wave patterns. As the electric field strength alone a standing wave may fluctuate over a wide range, the output of a mobile antenna which responds only to the electric field would fluctuate accordingly and exhibit spatial fading as it moves about. This phenomenon constitutes a serious problem in vehicle communication since at points of a minimum electric field intensity the resultant signal may fall below the noise level and therefore make communication impossible. Similar problems arise in radio communication with and between low-flying aircrafts.

J. R. Pierce has suggested the use of a three-antenna system which consists of a vertical electric dipole or unipole responding to the electric field and a pair of loop antennas responding to two perpendicular components of the magnetic field [1].

---

*This part has been submitted to the IEEE Transactions on Vehicular Technology and will be published in the May 1972 issue.

This energy density antenna system is one of means for combatting this spatial fading phenomenon.

II. THE SLOT-UNIPOLE ENERGY DENSITY ANTENNA SYSTEM

Assume that a mobile unit is to receive a vertically polarized wave. The electric field then has a z-component, $\bar{E} = \hat{z}E_z$; it can be detected by a vertical unipole. The magnetic field, being normal to the electric field, in general has both x- and y-components, $\bar{H} = \hat{x}H_x + \hat{y}H_y$. The crossed slots shown in Fig. 1 will detect the H_x and H_y components [3]. Note that the reference axes in the xy-plane are arbitrary, as an $\bar{H}$ vector in the xy-plane can always be decomposed into two perpendicular components.

In Fig. 2 is shown a processing circuit, which three square-law detectors are used. The detectors process and effectively square the outputs of the three component antennas. The output of the summing amplifier is then proportional to the energy density of the wave intercepted by the slot-unipole antenna system. If W denotes the energy density, the constants of the square-law detectors and/or the summing amplifier are to be adjusted such that

$$W = \frac{1}{2}\left(\varepsilon_o E_z \cdot E_z^* + \mu_o H_x \cdot H_x^* + \mu_o H_y \cdot H_y^*\right) \tag{1}$$

or

$$W = \frac{1}{2}\left(\varepsilon_o |E_z|^2 + \mu_o |H_x|^2 + \mu_o |H_y|^2\right)$$

$$= \frac{1}{2}\left(\varepsilon_o |E|^2 + \mu_o |H|^2\right) \tag{2}$$

where ε_o and μ_o are the permittivity and permeability of free space respectively. As will be shown in Section IV, the range of variation of W is smaller than that for the magnitude of the electric field alone in all situations. The standing-wave pattern of the electric field goes through maxima and minima. In a nondissipative medium, the minima are zero, making signal reception with only a vertical antenna impossible.

In comparison with the unipole-and-loops arrangement, the slot-unipole antenna system has several advantages. First, a slot antenna can be matched easily by an off-set feeder line. Second, a slot antenna is more suitable for installation in high-speed vehicles such as aircrafts. Third, the coupling between the slots and the unipole antenna is very small. Fourth, when the diameter of a quarter-wavelength unipole equals one-half of the slot width, the unipole and slot antennas have the same frequency bandwidth and the same impedance characteristics.

III. REFLECTING-PLANE MODEL ANALYSIS

We now use a simple reflecting-plane model to analyze the response of energy-density antennas. An infinite vertical conducting plane as shown in Fig. 3 is used to simulate the side of a tall building or a mountain. The electric field of a vertically polarized plane wave incident on a mobile antenna which moves with a velocity $\bar{v}$ is

$$\bar{E}_i = \hat{z}E_{iz} = \hat{z}A \exp\{j[\omega t - \bar{k}_o \cdot (\bar{r} + \bar{v}t)]\} . \qquad (3)$$

Similarly, the magnetic field is

$$\bar{H}_i = -\frac{A}{\eta_o}[\hat{x} \sin \phi + \hat{y} \cos \phi] \exp\{j[\omega t - \bar{k}_o \cdot (\bar{r} + \bar{v}t)]\} \qquad (4)$$

where k_o and η_o are, respectively, the wavenumber and the intrinsic

impedance of free space; that is, $k_o = \omega\sqrt{\mu_o\varepsilon_o} = 2\pi/\lambda$ and $\eta_o = \sqrt{\mu_o/\varepsilon_o}$. On reflection from the perfectly conducting plane, we can readily write down the expressions for the reflected electric and magnetic fields by requiring the total tangential electric field to vanish at $z = 0$. The three resultant field components at the moving vehicle are readily found to be [3]:

$$E_z = j2A \sin \psi(t) \cdot \exp[-j\xi(t)] \tag{5}$$

$$H_x = -\frac{2A}{\eta_o} A \sin \phi \cos \psi(t) \cdot \exp[-j\xi(t)] \tag{6}$$

$$H_y = -j\frac{2A}{\eta_o} \cos \phi \sin \psi(t) \cdot \exp[-j\xi(t)] \tag{7}$$

where

$$\psi(t) = k_o(y + vt \sin \alpha) \sin \phi \tag{8}$$

$$\xi(t) = k_o(x + vt \cos \alpha) \cos \phi - \omega t \tag{9}$$

and α is the angle which the vehicle motion makes with the x-axis.

Substituting (5)-(7) in (2), we obtain the expression for energy density to which the output of the processing circuit following the slot-unipole antenna system will be proportional.

$$W = 2A^2\varepsilon_o[(1 + \cos^2\phi) \sin^2\psi(t) + \sin^2\phi \cos^2\psi(t)], \tag{10}$$

If only a vertical unipole is used to receive the electric field, the output of the square-law detector will be

$$W_E = \frac{1}{2} \varepsilon_o |E_z|^2$$

$$= 2A^2\varepsilon_o \sin^2\psi(t) \tag{11}$$

or, using (8),

$$W_E = A^2\varepsilon_o\{1 - \cos[2k_o(y + vt \sin \alpha) \sin \phi]\} . \tag{12}$$

IV. INTERPRETATION OF RESULTS

In vehicular communication we are interested in the variation of signal output as a function of vehicle motion. It is evident from (10) and (11) that the response of both the energy-density antenna system and the single vertical unipole depends on $\psi(t)$ which is a function of the instantaneous normal distance of the vehicle from the reflecting plane. In addition, W in (10) depends also on the angle ϕ. Two interesting limiting conditions can be noted immediately.

1. When vehicle motion is parallel to the conducting plane (wall): $\alpha=0$, $\psi=k_o y$ is a constant, both W and W_E are independent of t and the signal output does not fluctuate in either case.
2. When the incident wave is normal to the conducting plane*: $\phi=\pi/2$ and, from (10), $W=2A^2\varepsilon_o$ which is a constant. Hence the signal output from the energy-density antenna system is constant and is independent of the magnitude or direction of vehicle velocity, while W_E remains a function of v,t, and α.

In order to determine the range of signal variation and the fading frequency, it is convenient to rewrite (10) and (11) as

$$W = 2A^2\varepsilon_o[1 - \frac{1}{2}(1 + \cos 2\phi)\cos 2\psi(t)] \qquad (12)$$

and

$$W_E = 2A^2\varepsilon_o \cdot \frac{1}{2}[1 - \cos 2\psi(t)] \, . \qquad (13)$$

From (12) and (13), we note further the following results.

---

*Note that (9), (10) and (11) are not useful for interpreting the situation for $\phi=0$ (which would make $\psi(t)=0$ in (8)) when the incident wave is parallel to the conducting plane. The reason is that there would be no reflection at $\phi=0$. Obviously, neither W nor W_E would be zero for an incident wave parallel to the x-axis.

3. Since cosine is a periodic function with a period 2π, both W in (12) and W_E in (13) are seen to be periodic. The fading frequency, f_d, can be found in either case by setting the variable part of $2\psi(t)$ to equal 2π. Hence, from (8),

$$k_o v(\Delta t)\,|\sin\alpha \sin\phi| = \pi \tag{14}$$

or

$$f_d = \frac{1}{\Delta t} = \frac{2v}{\lambda}\,|\sin\alpha \sin\phi|. \tag{15}$$

Apart from the obvious fact that the fading frequency is higher for higher velocity and shorter wavelength, (15) states that f_d increases with both an increasing α and an increasing ϕ. The maximum value of f_d occurs when both α and ϕ equal $\pi/2$.

$$\text{Max. } f_d = \frac{2v}{\lambda} \tag{16}$$

which corresponds to a traveled distance of a half-wavelength of the incident wave, as expected.

4. From (12), we obtain the range of variation of the normalized output from the energy-density antenna, $W/2A^2\varepsilon_o$:

$$\frac{1}{2}(1 - \cos 2\phi) \leq \frac{W}{2A^2\varepsilon_o} \leq \frac{1}{2}(3 + \cos 2\phi)\ . \tag{17}$$

The right and left sides of (17) have been plotted versus the angle ϕ in Fig. 3, as the upper and lower bounds for W. A dB-scale is used for the amplitudes, the reference amplitude (zero dB) being unity. The range between the upper and lower curves at a given ϕ represents the range of maximum variation of W for all possible vehicle location, velocity, and direction of motion. It is seen that the range decreases rapidly as ϕ increases. Of course, the maximum range of amplitude variation for W_E is ∞ dB for all ϕ.

V. CONCLUSION AND DISCUSSION

An energy-density antenna that samples the electromagnetic energy density provides a way for combating the spatial fading phenomenon which is encountered in vehicular communication. The principle of operation and the advantages of a slots-and-unipole energy-density antenna system have been discussed. Using a simple reflecting-plane model, the signal output from the energy-density antenna system and that from a single unipole antenna are obtained as expressions which depend on the angle of incidence and the magnitude and the direction of vehicle velocity in a general way. From these general expressions the fading frequency and the maximum range of output variation are found. The extent of amplitude fluctuation for the energy-density antenna system is always smaller than that for the single antenna. When the incident wave is normal to the reflecting plane, the energy-density antenna yields a constant output regardless of the magnitude or direction of the velocity of the moving vehicle.

In situations where there exist more than one reflecting wall or mountain, the resultant field would be the sum of the incident field and two or more reflected fields. Moreover, multiple reflections may occur, making the problem more complicated. In the most general case, the problem becomes a statistical one [1,2], and one can only discuss the probability distributions and average properties of the output signal. Nevertheless, the simple model affords a first-order analysis and an understanding of the response characteristics of the energy-density antenna system.

VI. REFERENCES

[1] E. N. Gilbert, "Energy reception for mobile radio," Bell Sys. Tech. Jour., vol. 44, pp. 1779-1803, October 1965.

[2] W.C.-Y. Lee, "Statistical analysis of the level crossings and duration of fades of the signal from an energy density mobile radio antenna," Bell Sys. Tech. Jour., vol. 46, pp. 417-448, February 1967.

[3] K. Itoh and T. Matsumoto, "A proposal of a new type of energy density mobile radio antenna" (in Japanese), Engineering research report No. 53, Hokkaido University, Sapporo, Japan, March 1969.

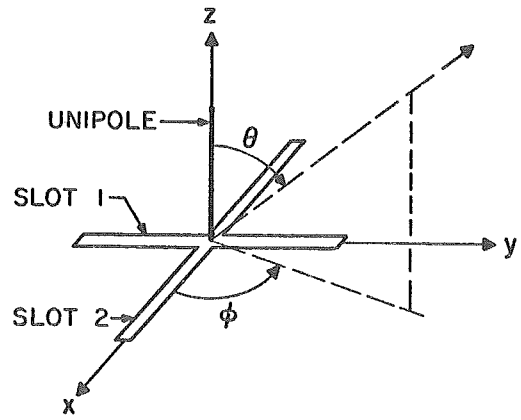

Figure 1. A slot-unipole antenna system.

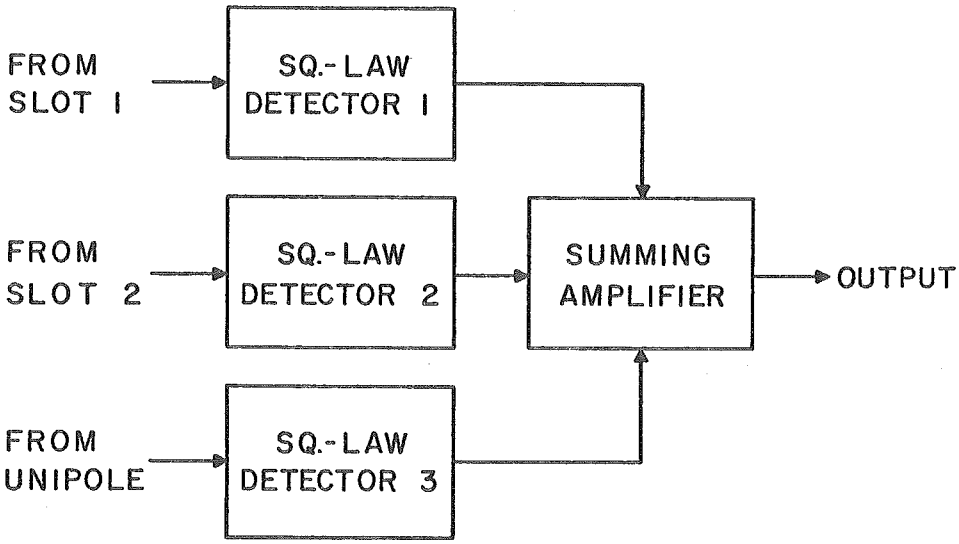

Figure 2. Processing circuit for energy-density antenna.

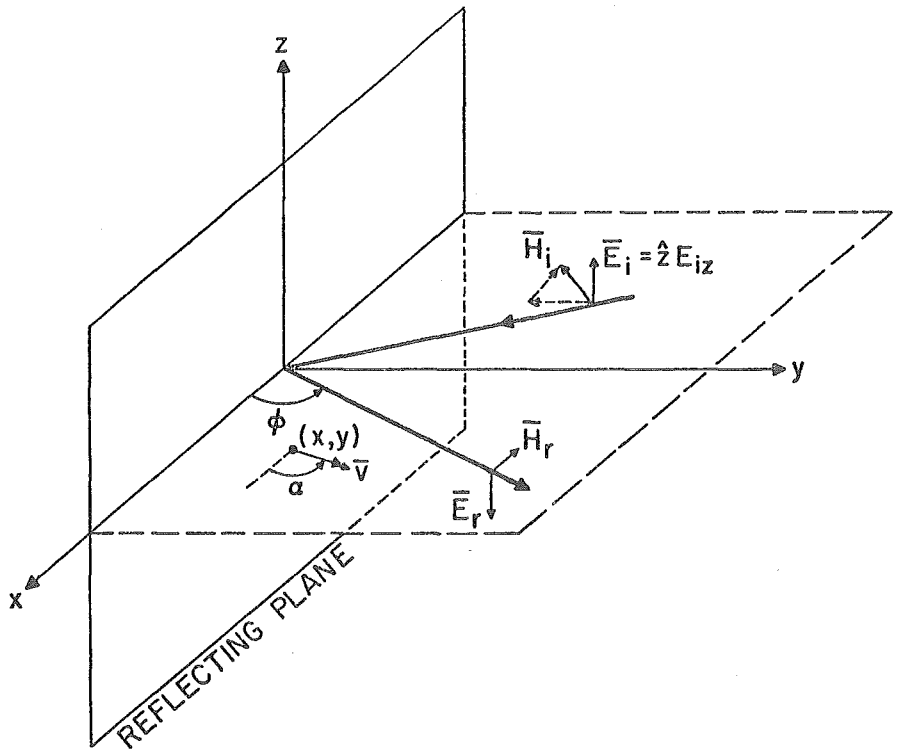

Figure 3. Reflecting-plane model.

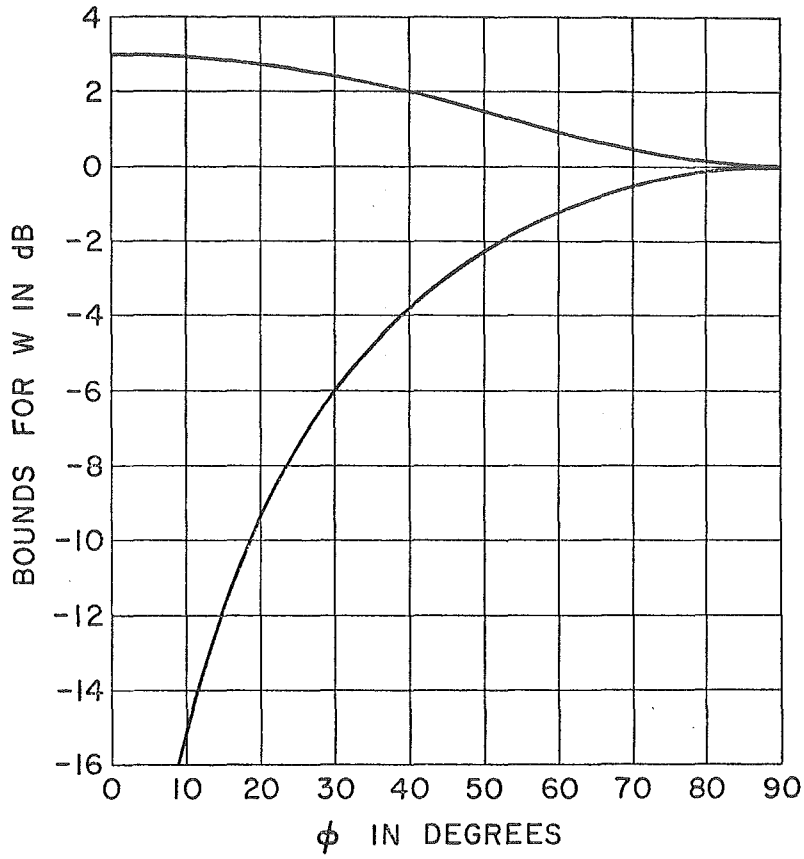

Figure 4. Bounds of energy density.

PART B* ANTENNA WITH A STEERABLE CARDIOID PATTERN

I. INTRODUCTION

By combining slot-monopole antennas with a processing circuit like Fig. 1 and 2, we can make a unit that has a cardioid-shaped pattern that is steerable without mechanical motion. Such antenna system has found important applications in direction-finding [1].

II. PRINCIPLE OF OPERATION

With the indicated spherical coordinates in Fig. 1, the pattern of the vertical antenna is omnidirectional in ϕ. For a quarter-wavelength monopole over a conducting ground plane, the normalized pattern function in any plane containing the z-axis is

$$E_M = \frac{\cos(\frac{\pi}{2}\cos\theta)}{\sin\theta} . \tag{1}$$

If the slot antennas are a half-wavelength long and very narrow, then the normalized pattern function for slot 1 in a plane containing the z-axis [2]

$$E_{s1} = \frac{\cos(\frac{\pi}{2}\sin\theta\cos\phi)}{1-\sin^2\theta\cos^2\phi}\sin\phi \tag{2}$$

and that for slot 2 is

$$E_{s2} = -\frac{\cos(\frac{\pi}{2}\sin\theta\sin\phi)}{1-\sin^2\theta\cos^2\phi}\cos\phi . \tag{3}$$

Note that E_{s1} in Eq. (2) corresponds to the θ-component of the radiated electric field when slot 1 is excited with a cosinusoidal aperture field in the positive y-direction and E_{s2} in Eq. (3) corresponds to that when

---

*This part has been accepted for publication in the IEEE Transactions on Aerospace and Electronic Systems.

slot 2 is excited with a cosinusoidal aperture field in the negative x-direction. These chosen directions are arbitrary and depend on how the feed lines are connected to the slots.

When the outputs from the monopole and slot 1 are combined, we obtained from Eqs. (1) and (2)

$$E_{Ms1} = \frac{\cos(\frac{\pi}{2}\cos\theta)}{\sin\theta} + \frac{\cos(\frac{\pi}{2}\sin\theta\cos\phi)}{1-\sin^2\theta\cos^2\phi}\sin\phi \ . \tag{4}$$

In the xy-plane, $\theta = \pi/2$, Eq. (4) reduces to

$$E_{Ms1}\Big|_{z=0} = 1 + \frac{\cos(\frac{\pi}{2}\cos\phi)}{\sin\phi} \tag{5}$$

and in the yz-plane Eq. (4) becomes

$$E_{Ms1}\Big|_{x=0} = \begin{cases} \dfrac{\cos(\frac{\pi}{2}\cos\theta)}{\sin\theta} + 1 \ , & \phi = +\pi/2 \\ \dfrac{\cos(\frac{\pi}{2}\cos\theta)}{\sin\theta} - 1 \ , & \phi = -\pi/2 \ . \end{cases} \tag{6}$$

Equations (5) and (6) have been plotted in Fig. 2 where it is seen that the patterns in both xy- and yz-planes are shaped like a cardioid. These are fixed space patterns.

Similarly the combined output of the monopole and slot 2 is, from Eqs. (1) and (3),

$$E_{Ms2} = \frac{\cos(\frac{\pi}{2}\cos\theta)}{\sin\theta} - \frac{\cos(\frac{\pi}{2}\sin\theta\sin\phi)}{1-\sin^2\theta\sin^2\phi}\cos\phi \ . \tag{7}$$

Fixed cardioid-like patterns are also obtained from E_{Ms2} in Eq. (7) in the xy- and xz-planes.

In order to obtain a steerable cardioid-like pattern, we use the processing circuit in Fig. 3. The outputs from slots 1 and 2 are amplified by factors A_1 and A_2 and phase-shifted by angles ψ_1 and ψ_2 respectively before being combined with the output from the monopole. We have

$$E_o(\theta,\phi) = E_M + E_{s1}A_1 e^{j\psi_1} + E_{s2}A_2 e^{j\psi_2}$$

$$= \frac{\cos(\frac{\pi}{2}\cos\theta)}{\sin\theta} + \frac{\cos(\frac{\pi}{2}\sin\theta\cos\phi)}{1-\sin^2\theta\cos^2\phi}\alpha_1\sin\phi$$

$$- \frac{\cos(\frac{\pi}{2}\sin\theta\sin\phi)}{1-\sin^2\theta\sin^2\phi}\alpha_2\cos\phi \qquad (8)$$

where

$$\alpha_1 = A_1 e^{j\psi_1} \qquad (9)$$

$$\alpha_2 = A_2 e^{j\psi_2} \qquad (10)$$

In the xy-plane, $\theta = \pi/2$, Eq. (8) becomes

$$E_o(\tfrac{\pi}{2},\phi) = 1 + \frac{\cos(\frac{\pi}{2}\cos\phi)}{\sin\phi}\alpha_1 - \frac{\cos(\frac{\pi}{2}\sin\phi)}{\cos\phi}\alpha_2 . \qquad (11)$$

The combined output $E_o(\frac{\pi}{2},\phi)$ will have a null at an angle $\phi = \phi_{null}$ when the azimuth angle satisfies the following two relations:

$$E_o(\tfrac{\pi}{2},\phi_{null}) = 0 \qquad (12)$$

and

$$\left[\frac{\partial}{\partial\phi} E_o(\tfrac{\pi}{2},\phi)\right]_{\phi=\phi_{null}} = 0 . \qquad (13)$$

From Eqs. (11), (12), and (13), we can find α_1 and α_2. Since the coefficients of α_1 and α_2 are real, the values of α_1 and α_2 for $\phi = \phi_{null}$

will be real, and ψ_1 and ψ_2 will be either 0 or π. The locus of ϕ_{null} has been computed and plotted on the $\alpha_1\alpha_2$-plane as the solid curve in Fig. 4. The following relation between ψ_1, ψ_2 and the ranges of ϕ_{null} is noted.

Table 1

Relation between ϕ_{null}, ψ_1, and ψ_2

ϕ_{null} / ψ_1,ψ_2	0°-90°	90°-180°	180°-270°	270°-360°
ψ_1	π	π	0	0
ψ_2	0	π	π	0

The direction of the pattern maximum, ϕ_{max}, can be found from the following two relations:

$$\left[\frac{\partial}{\partial\phi} E_o\left(\frac{\pi}{2},\phi\right)\right]_{\phi=\phi_{max}} = 0 \tag{14}$$

and

$$\left[\frac{\partial^2}{\partial\phi^2} E_o\left(\frac{\pi}{2},\phi\right)\right]_{\phi=\phi_{max}} < 0 \tag{15}$$

Numerical computation has shown that

$$\phi_{max} \cong \phi_{null} + \pi \tag{16}$$

is accurate down to the second decimal place; hence, the pattern maximum always occurs on the opposite side of the pattern null and has an approximate magnitude of 2.

If the crossed slots are not a half-wavelength long but are very short compared to a wavelength, they can be considered as magnetic

dipoles and the combined pattern in the xy-plane, $E_o(\frac{\pi}{2},\phi)$ in Eq. (11), can be approximated by

$$E_o(\tfrac{\pi}{2},\phi) \simeq 1 + \alpha_1 \sin\phi - \alpha_2 \cos\phi$$

$$= 1 + \sin(\phi - \delta) \tag{17}$$

where $\sqrt{\alpha_1^2 + \alpha_2^2}$ has been set to unity and

$$\delta = \tan^{-1}(\alpha_2/\alpha_1) \tag{18}$$

We note from the discussion following Eq. (13) that both α_1 and α_2 are real. The locus of ϕ_{null} in this case is found by setting $\sin(\phi-\delta)$ in Eq. (17) to equal -1. We have

$$\delta = \phi_{null} + 90° \tag{19}$$

and the locus is a circle, shown dashed in Fig. 4. The pattern in the xy-plane for vertically polarized waves obtained with a monopole and crossed magnetic dipoles remains a true cardioid as it is steered through space.

III. CHARACTERISTICS OF SYNTHESIZED PATTERN

We now examine the synthesized pattern of the combined output of the slots-and-monopole antenna. Since $E_o(\theta,\phi)$ in Eq. (8) depends on the angles θ and ϕ in a complicated way, it is expected that E_o as a function of θ in a constant-ϕ plane will depend on the value of ϕ. We assume that α_1 and α_2 are always adjusted so that a cardioid-type pattern is obtained in the xy-plane. The patterns in vertical planes with $\phi=\phi_{null}$ on one side and $\phi=\phi_{max}$ on the other are plotted in Fig. 5 for several values of ϕ_{null}. It is interesting to note that the patterns differ very little as

ϕ_{null} is changed over a wide range. This near constancy in the vertical pattern makes it an easy matter to estimate the so-called "standard wave error" [1] in direction-finding relative to the elevation angle of the incoming signal.

The pattern in the xy-plane for vertically polarized waves is the pattern of importance in direction-finding. This is the graph of Eq. (11) with the weighting factors α_1 and α_2 properly adjusted in accordance with Fig. 4 to yield a pattern null. Several such patterns have been plotted in Fig. 6. We note that the horizontal patterns are all cardioid-like and that they are symmetrical with respect to the direction of maximum signal for $\phi_{null} = 0°$, 45°, and 90°. At intermediate values of ϕ_{null} the pattern is slightly asymmetrical, although ϕ_{max} and ϕ_{null} always occur in nearly opposite directions. Since the pattern of a half-wavelength slot is more directive than that of a small loop used in the monopole-and-loops arrangement, sharper nulls are obtained than the null of a true cardioid. Sharper nulls mean more accurate direction-finding.

In Fig. 7 the half-power beamwidth of the horizontal pattern is plotted as a function of ϕ_{null}. This beamwidth is quite wide, being nearly constant at 140° when the pattern is scanned between $\phi_{null} = 30°$ and 60°. The narrowest beamwidth of 122° occurs when $\phi_{null} = 0°$ and 90°. When crossed magnetic dipoles are used in conjunction with a monopole to obtain true cardioid patterns, a constant beamwidth of 131° is obtained. This is indicated by the dashed line in Fig. 7.

IV. CONCLUSION

A vertical monopole and two crossed slots form an antenna unit whose combined output can be processed to yield a cardioid-shaped horizontal pattern for vertically polarized waves. This cardioid-shaped pattern is steerable in the azimuth direction by properly weighting the outputs of the crossed slots. The locus for determining these weighting factors for any desired null direction has been given. Both the shape and the half-power beamwidth of the steerable pattern have also been examined. It appears that this combination antenna unit offers important advantages in direction-finding applications, especially at microwave frequencies. It is also useful in situations where broad-beam reception coupled with interference suppression in a particular direction is desired. The directive properties of such units suggest their possible use as the elements in an antenna array.

V. REFERENCES

[1] H. Jasik, Antenna Engineering Handbook, Chapter 28, McGraw-Hill Book Co., 1961.

[2] R. E. Collin and F. J. Zucker, Antenna Theory, Part 1, Chapter 14, McGraw-Hill Book Co., 1969.

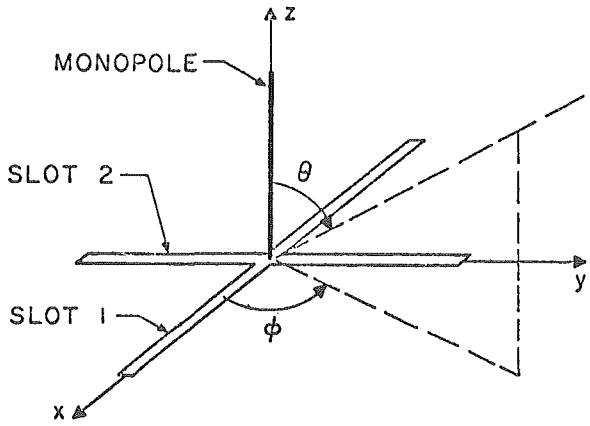

Fig. 1. A slots-and-monopole antenna unit.

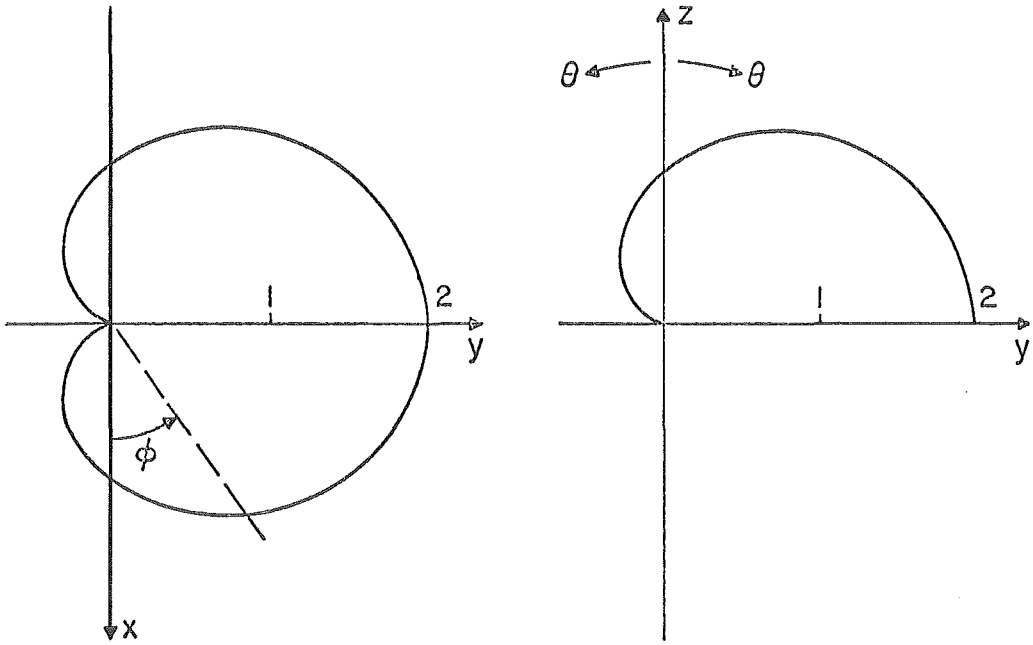

(a) in xy-plane (b) in yz-plane

Fig. 2. Combined output of monopole and slot 1.

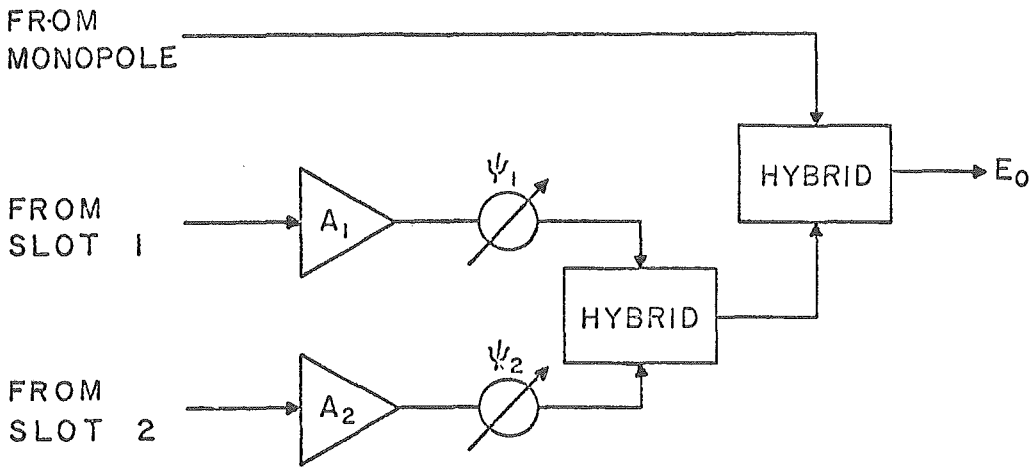

Fig. 3. Processing circuit for pattern control.

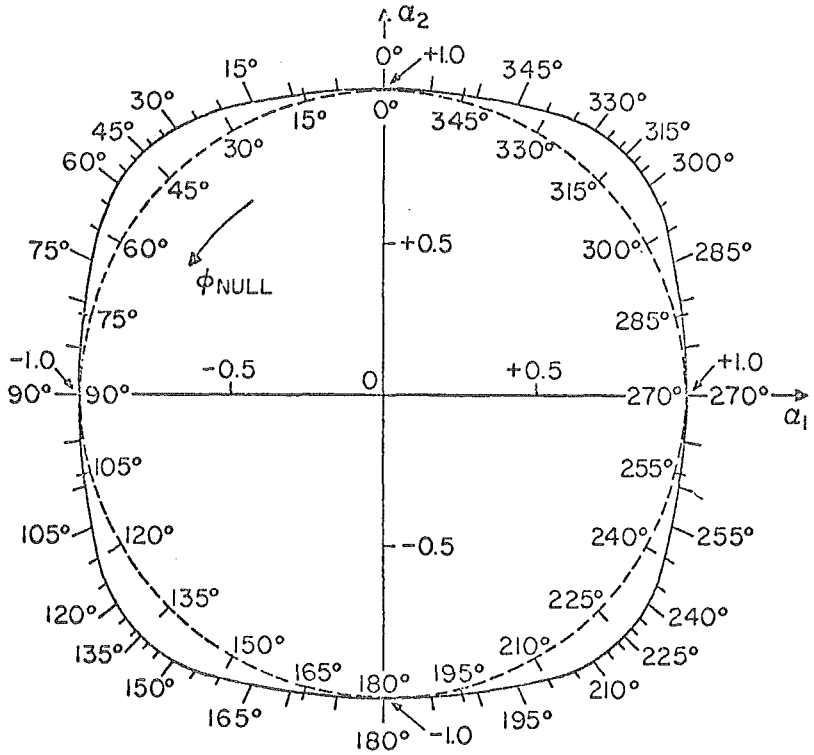

Fig. 4. Loci for ϕ_{null} in $\alpha_1\alpha_2$-plane

——— Monopole and crossed λ/2 slots

– – – – – Monopole and crossed magnetic dipoles.

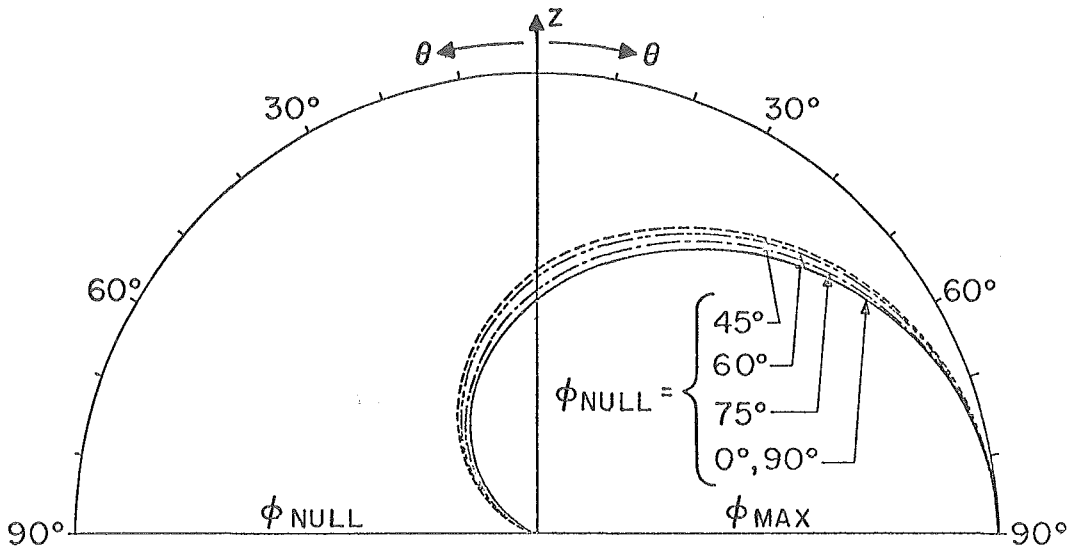

Fig. 5. Variation of E_o in vertical plane containing z-axis and ϕ_{null}-ϕ_{max}

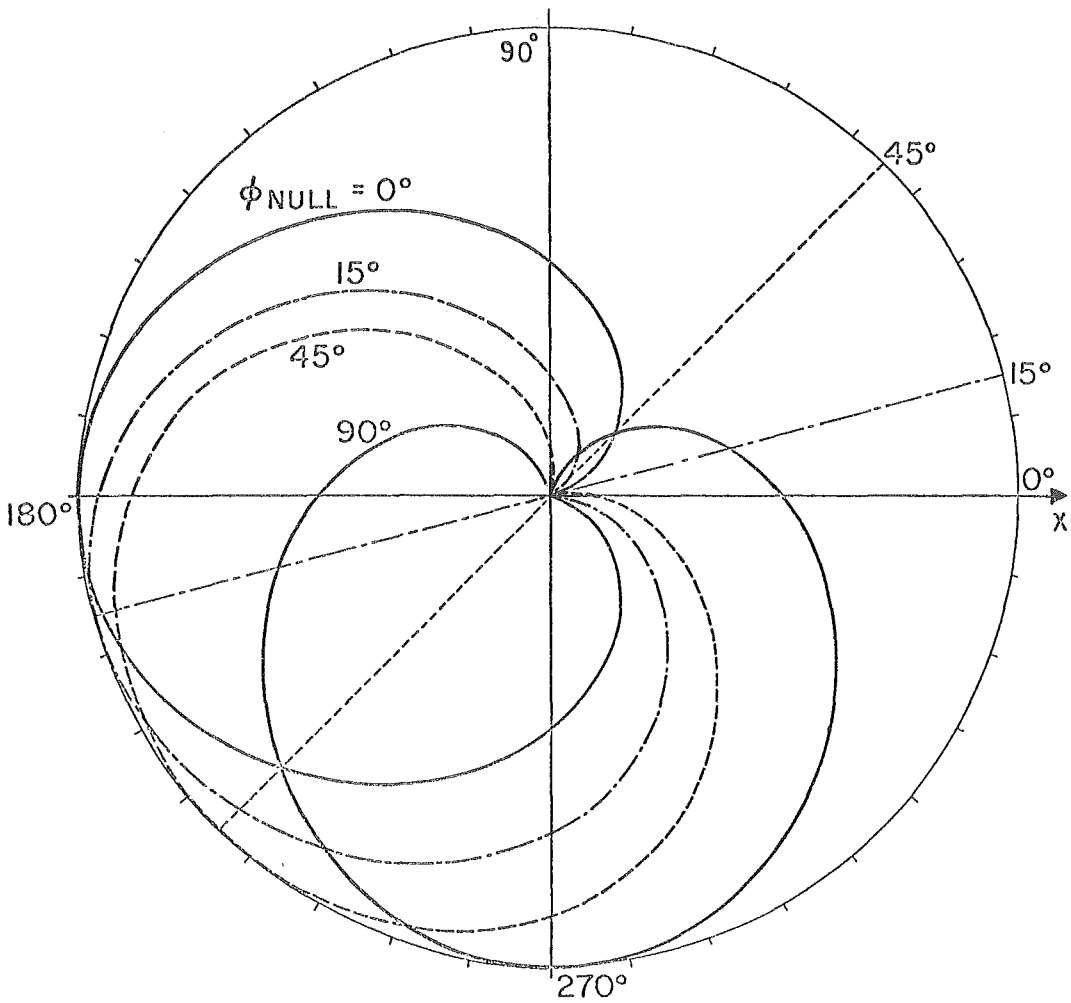

Fig. 6. Horizontal patterns of slots-and-monopole antenna

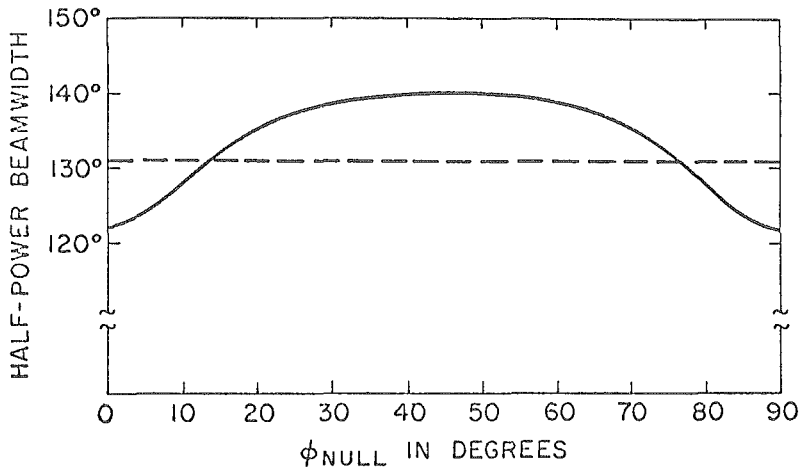

Fig. 7. Half-power beamwidth of horizontal pattern as a function of null direction.

——— Monopole and crossed λ/2 slots

– – – – Monopole and crossed magnetic dipoles.